Eur. Phys. J. C 12, 587–593 (2000)
Digital Object Identifier (DOI) 10.1007/s100520000179

THE EUROPEAN PHYSICAL JOURNAL C

High-twist contribution to the longitudinal structure function $F_{\rm L}$ at high x

S.I. Alekhin

Institute for High Energy Physics, Protvino, 142284, Russia (e-mail: alekhin@mx.ihep.su)

Received: 21 April 1999 / Revised version: 17 June 1999 /
Published online: 27 January 2000 –

Abstract. We perform the NLO QCD fit to the combined deep inelastic scattering (DIS) data at high x from the SLAC, BCDMS, and NMC collaborations. The model-independent x shape of the high-twist contribution to structure function $F_{\rm L}$ is extracted. The twist-4 contribution to $F_{\rm L}$ is found to be in a qualitative agreement with the predictions of the infrared renormalon model. The twist-6 contribution exhibits a weak trend to negative values, although on the whole, it is compatible with zero within the errors.

1 Introduction

It is well known that on the basis of the operator product expansion, the deep inelastic scattering (DIS) cross sections can be split into the leading-twist (LT) and the high-twist (HT) contributions. Up to now, the LT contribution has been fairly understood from both the theoretical and experimental points of view. The HT contribution is not so well explored. The theoretical investigations of the HT contribution meet with difficulties because in the region where this contribution is most important, the perturbative QCD calculations cannot be applied. There are only semiqualitative models for the calculation of the HT contribution. These models are often based on the phenomenological considerations and contain adjusted parameters, which are to be determined from experimental data. Unfortunately, the relevant experimental data, especially on the longitudinal structure function $F_{\rm L}$, are sparse and come from different experiments; they are therefore difficult to interpret. There are estimations of the twist-4 contribution to structure function F_2 [1–4] obtained from fits to SLAC-BCDMS-NMC data [5–7]. Estimations of the HT contributions to F_3 were obtained in [8,9] from the fit to CCFR data [10]. These estimations are model-independent, i.e., they do not imply any x dependence of HT, hence a phenomenological formula can be easily fitted to them. As to the experimental data on HT contribution to $F_{\rm L}$, they are available only from the QCD-motivated fits to the world data on the structure function $R = \sigma_{\rm L}/\sigma_{\rm T}$. The first fit of this kind was presented in [11] and was recently renewed in [12] with inclusion of the new data from experiments SLAC-E-143 and SLAC-E-140X. The world data on R were also analyzed by the use of a QCD-based model accounting for HT contribution [13]. Since some models predict the HT contribution to structure function $F_{\rm L}$, the comparison of those models with data requires extraction of the HT contribution to $F_{\rm L}$ from the data on HT contribution to R and F_2. This causes problems with interpolation between the data points and error propagation. In addition, the HT contributions to R obtained in all these fits are model-dependent, i.e., they *a priori* suppose a certain x dependence of HT.

Table 1. The number of data points (NDP) and the number of independent systematic errors (NSE) for the analyzed data sets

Experiment	NDP (proton)	NDP (deuterium)	NSE
BCDMS	223	162	9
E-49A	47	47	3
E-49B	109	102	3
E-61	6	6	3
E-87	90	90	3
E-89A	66	59	3
E-89B	70	59	3
E-139	–	16	3
E-140	–	31	4
NMC	30	30	13
TOTAL	641	602	47

2 Extraction of the HT contribution to $F_{\rm L}$

In this paper, we present the results of DIS data analysis aimed at obtaining the estimation of the model-independent HT contribution to $F_{\rm L}$. The work is the continuation of our previous study [3], where the estimation of the HT contribution to F_2 has been obtained. Our consideration is limited by the region of $x > 0.3$, where the nonsinglet

approximation is valid. A data cut $x \le 0.75$ was made to minimize influence of nuclear effects in deuterium. A Q^2 region spanned by the data remaining after the cuts is 1–230 GeV^2. At the first stage of the analysis the ansatz used in this work is essentially the same as in [3]. The fitted formula for F_2 are taken within the NLO QCD approximation with inclusion of target mass correction (TMC) [14] and twist-4 contribution in a factorized form:

$$F_2^{\rm (p,d),HT}(x,Q) = F_2^{\rm (p,d),TMC}(x,Q)\left[1+\frac{h_2^{\rm (p,d)}(x)}{Q^2}\right],$$

$$F_2^{\rm (p,d),TMC}(x,Q) = \frac{x^2}{\tau^{3/2}}\frac{F_2^{\rm (p,d),LT}(\xi,Q)}{\xi^2}+$$

$$+6\frac{M^2}{Q^2}\frac{x^3}{\tau^2}\int_\xi^1 {\rm d}z\frac{F_2^{\rm (p,d),LT}(z,Q)}{z^2},$$

where $F_2^{\rm (p,d),LT}(x,Q)$ are the LT terms,

$$\xi = \frac{2x}{1+\sqrt{\tau}}, \quad \tau = 1+\frac{4M^2x^2}{Q^2},$$

M is the nucleon mass, and x and Q^2 are regular lepton scattering variables. The LT structure functions of protons and neutrons were parametrized at the initial value of $Q_0^2 = 9$ GeV^2 as follows:

$$F_2^{\rm p,n}(x,Q_0) = A_{\rm p,n}x^{a_{\rm p,n}}(1-x)^{b_{\rm p,n}}\frac{2}{N_{\rm p,n}}$$

Here the conventional normalization factors $N_{\rm p}$ and $N_{\rm n}$ are

$$N_{\rm p,n} = \int_0^1 {\rm d}x x^{a_{\rm p,n}-1}(1-x)^{b_{\rm p,n}}.$$

These distributions were evolved in the NLO QCD approximation within the modified minimal subtraction ($\overline{\rm MS}$) factorization and renormalization schemes. The functions $h_2^{\rm (p,d)}(x)$ were parametrized in the model-independent way: Their values at $x = 0.3, 0.4, 0, 5, 0.6, 0.7, 0.8$ were fitted, and between these points the functions were linearly interpolated.

As compared to [3], we have added the NMC data [7] to the analysis (30 points on proton and 30 points on deuterium targets). The number of data for each experiment and target are given in Table 1. We accounted for point-to-point correlations of data due to systematic errors as we did in our previous papers [3,9,15]. The systematic errors were convoluted into a covariance matrix

$$C_{ij} = \delta_{ij}\sigma_i\sigma_j + f_if_j(\mathbf{s}_i^K\cdot\mathbf{s}_j^K),$$

where vectors $\mathbf{s}_i^K$ contain the systematic errors; index K runs through the data subsets, which are not correlated with each other; and i and j run through the data points of these data subsets. A minimized functional has the form

$$\chi^2 = \sum_{K,i,j}(f_i/\xi_K - y_i)E_{ij}(f_j/\xi_K - y_j),$$

Table 2. The results of the fits with the factorized parametrization of HT. The parameters ξ describe the renormalization of old SLAC data; $h^{\rm p,d}_{2,(3,4,5,6,7,8)}$ are the fitted values of the HT contribution at $x = 0.3, 0.4, 0.5, 0.6, 0.7, 0.8$. For the description of the columns, see the text

	1	2
$A_{\rm p}$	0.516 ± 0.022	0.514 ± 0.021
$a_{\rm p}$	0.765 ± 0.028	0.766 ± 0.028
$b_{\rm p}$	3.692 ± 0.032	3.690 ± 0.032
$A_{\rm n}$	4.8 ± 4.1	4.8 ± 3.9
$a_{\rm n}$	0.118 ± 0.097	0.119 ± 0.095
$b_{\rm n}$	3.51 ± 0.11	3.51 ± 0.11
$\alpha_{\rm s}(M_{\rm Z})$	0.1180 ± 0.0017	0.1187 ± 0.0016
$h^{\rm p}_{2,3}$	-0.120 ± 0.017	-0.122 ± 0.017
$h^{\rm p}_{2,4}$	-0.046 ± 0.025	-0.054 ± 0.025
$h^{\rm p}_{2,5}$	0.059 ± 0.043	0.043 ± 0.042
$h^{\rm p}_{2,6}$	0.392 ± 0.076	0.363 ± 0.074
$h^{\rm p}_{2,7}$	0.82 ± 0.13	0.77 ± 0.12
$h^{\rm p}_{2,8}$	1.54 ± 0.25	1.47 ± 0.24
$h^{\rm d}_{2,3}$	-0.123 ± 0.018	-0.125 ± 0.018
$h^{\rm d}_{2,4}$	-0.003 ± 0.026	-0.012 ± 0.025
$h^{\rm d}_{2,5}$	0.162 ± 0.043	0.145 ± 0.042
$h^{\rm d}_{2,6}$	0.439 ± 0.076	0.410 ± 0.073
$h^{\rm d}_{2,7}$	0.79 ± 0.12	0.75 ± 0.11
$h^{\rm d}_{2,8}$	1.87 ± 0.26	1.81 ± 0.25
$\xi_{{\rm p},49A}$	1.016 ± 0.018	1.016 ± 0.016
$\xi_{{\rm d},49A}$	1.006 ± 0.017	1.008 ± 0.015
$\xi_{{\rm p},49B}$	1.028 ± 0.018	1.028 ± 0.015
$\xi_{{\rm d},49B}$	1.012 ± 0.017	1.013 ± 0.015
$\xi_{{\rm p},61}$	1.021 ± 0.021	1.021 ± 0.019
$\xi_{{\rm d},61}$	1.004 ± 0.019	1.006 ± 0.018
$\xi_{{\rm p},87}$	1.025 ± 0.017	1.025 ± 0.015
$\xi_{{\rm d},87}$	1.012 ± 0.017	1.013 ± 0.015
$\xi_{{\rm p},89A}$	1.028 ± 0.021	1.029 ± 0.019
$\xi_{{\rm d},89A}$	1.004 ± 0.021	1.006 ± 0.019
$\xi_{{\rm p},89B}$	1.022 ± 0.017	1.021 ± 0.015
$\xi_{{\rm d},89B}$	1.007 ± 0.017	1.008 ± 0.015
$\xi_{{\rm d},139}$	1.009 ± 0.017	1.010 ± 0.015
χ^2/NDP	1178.9/1183	1258.4/1243

where $E_{i,j}$ is the inverse of $C_{i,j}$. The dimension of $\mathbf{s}_i^K$ differs for various data sets, the particular numbers for each experiment are given in Table 1. The factors ξ_K were introduced to allow for the renormalization of some data sets. In our analysis, these factors were released for the old SLAC experiments in view of possible normalization errors discussed in [16]. As for the E-140, BCDMS, and NMC data subsets, we fixed these factors at 1 and accounted for their published normalization errors in the general covariance matrix.

At the first stage of the analysis, we reduced all the F_2 data, including the BCDMS and NMC ones, to the com-

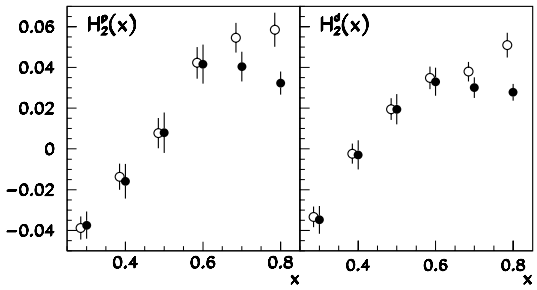

Fig. 1. The results of fits with different forms of HT contribution (full circles: additive; empty circles: factorized). For a better view, the points are slightly shifted to the left/right along the x axis

mon value of R from [11]. The results of the fit within this ansatz are given in Table 2, column 2. For comparison we also give the results of the analogous fit from [3], which was performed without the NMC data, in column 1. Addition of the NMC data increased the value of $\alpha_{\rm s}(M_{\rm Z})$, but within one standard deviation. On the whole, the figures from column 2 are compatible with the results of earlier analysis [3].

The next step of our analysis was to change the form of HT contribution from the factorized to an additive one:

$$F_2^{\rm (p,d),HT}(x,Q) = F_2^{\rm (p,d),TMC}(x,Q) + H_2^{\rm (p,d)}(x)\frac{1\ {\rm GeV}^2}{Q^2},$$

where $H_2^{\rm (p,d)}(x)$ are parametrized in the model-independent form analogously to $h_2^{\rm (p,d)}(x)$. We preferred switching to this form because for the factorized parametrization, the HT term contains a latent log factor and twist-6 contribution, originating from $F_2^{LT}(x,Q)$ and target mass corrections, respectively. In addition, this form is more convenient for comparison with some models' predictions. The results of the fit with additive HT parametrization are given in column 1 of Table 3 and in Fig. 1. For comparison we also give the value of $F_2^{\rm TMC}(x,Q)\cdot h_2(x)$ for the fit from column 2 of Table 2 with the factorized form of HT, calculated at $Q^2 = 2.5\ {\rm GeV}^2$. One can see that the switching of the form leads to a small decrease of HT terms at high x. Besides, the HT coefficients errors become smaller, while the errors of other parameters increase. We connect this effect with the fact that the additive HT form is not so constrained as the factorized one. It can also signal that the data are sensitive to deviation of the anomalous dimensions of twist-4 operators from zero (see in this connection [17]). However, as can be concluded from Fig. 1, the statistical significance of this deviation is poor, and more data at high x should be included in the analysis to clarify this point.

To extract $F_{\rm L}$, we have replaced the data on F_2 by the data on differential cross sections and fitted them using the formula

$$\frac{{\rm d}^2\sigma}{{\rm d}x{\rm d}y} = \frac{4\pi\alpha^2(s-M^2)}{Q^4}\left[\left(1-y-\frac{(Mxy)^2}{Q^2}\right)F_2^{\rm HT}(x,Q)+\right.$$

Table 3. The results of the fits with additive parametrization of HT. The parameters ξ describe the renormalization of old SLAC data; $H^{\rm p,d}_{2,(3,4,5,6,7,8)}$ and $H^{\rm p,d}_{\rm L,(3,4,5,6,7,8)}$ are the fitted values of the HT contribution at $x = 0.3, 0.4, 0.5, 0.6, 0.7, 0.8$. For the description of the columns, see the text

	1	2	3
$A_{\rm p}$	0.478 ± 0.021	0.485 ± 0.023	0.486 ± 0.022
$a_{\rm p}$	0.830 ± 0.034	0.816 ± 0.037	0.817 ± 0.035
$b_{\rm p}$	3.798 ± 0.043	3.791 ± 0.047	3.792 ± 0.045
$A_{\rm n}$	4.8 ± 4.5	4.8 ± 4.8	4.7 ± 4.7
$a_{\rm n}$	0.12 ± 0.11	0.12 ± 0.13	0.12 ± 0.12
$b_{\rm n}$	3.58 ± 0.14	3.59 ± 0.15	3.58 ± 0.14
$\alpha_{\overline{\rm MS}}(M_{\rm Z})$	0.1190 ± 0.0021	0.1170 ± 0.0021	0.1170 ± 0.0021
$H^{\rm p}_{2,3}$	-0.0374 ± 0.0067	-0.0303 ± 0.0068	-0.0273 ± 0.0067
$H^{\rm p}_{2,4}$	-0.0159 ± 0.0085	-0.0031 ± 0.0084	-0.0059 ± 0.0082
$H^{\rm p}_{2,5}$	0.0080 ± 0.0099	0.0176 ± 0.0096	0.0189 ± 0.0095
$H^{\rm p}_{2,6}$	0.0416 ± 0.0096	0.0497 ± 0.0095	0.0494 ± 0.0092
$H^{\rm p}_{2,7}$	0.0404 ± 0.0073	0.0529 ± 0.0077	0.0501 ± 0.0073
$H^{\rm p}_{2,8}$	0.0323 ± 0.0057	0.0376 ± 0.0081	0.0400 ± 0.0070
$H^{\rm d}_{2,3}$	-0.0348 ± 0.0068	-0.0205 ± 0.0066	-0.0221 ± 0.0065
$H^{\rm d}_{2,4}$	-0.0029 ± 0.0071	0.0057 ± 0.0069	0.0067 ± 0.0068
$H^{\rm d}_{2,5}$	0.0195 ± 0.0074	0.0274 ± 0.0071	0.0269 ± 0.0070
$H^{\rm d}_{2,6}$	0.0330 ± 0.0069	0.0381 ± 0.0068	0.0380 ± 0.0067
$H^{\rm d}_{2,7}$	0.0301 ± 0.0050	0.0363 ± 0.0051	0.0372 ± 0.0050
$H^{\rm d}_{2,8}$	0.0278 ± 0.0041	0.0354 ± 0.0061	0.0341 ± 0.0053
$H^{\rm p}_{\rm L,3}$	–	0.045 ± 0.027	–
$H^{\rm p}_{\rm L,4}$	–	0.036 ± 0.024	–
$H^{\rm p}_{\rm L,5}$	–	-0.009 ± 0.023	–
$H^{\rm p}_{\rm L,6}$	–	-0.012 ± 0.017	–
$H^{\rm p}_{\rm L,7}$	–	0.020 ± 0.013	–
$H^{\rm p}_{\rm L,8}$	–	0.004 ± 0.019	–
$H^{\rm d}_{\rm L,3}$	–	0.106 ± 0.016	0.095 ± 0.014
$H^{\rm d}_{\rm L,4}$	–	0.044 ± 0.013	0.049 ± 0.012
$H^{\rm d}_{\rm L,5}$	–	0.0343 ± 0.0089	0.031 ± 0.0087
$H^{\rm d}_{\rm L,6}$	–	0.009 ± 0.010	0.0068 ± 0.0094
$H^{\rm d}_{\rm L,7}$	–	0.0161 ± 0.0078	0.0195 ± 0.0069
$H^{\rm d}_{\rm L,8}$	–	0.021 ± 0.018	0.016 ± 0.013
$\xi_{{\rm p},49A}$	1.013 ± 0.016	1.017 ± 0.016	1.017 ± 0.016
$\xi_{{\rm d},49A}$	1.005 ± 0.015	1.007 ± 0.015	1.009 ± 0.015
$\xi_{{\rm p},49B}$	1.023 ± 0.015	1.039 ± 0.016	1.031 ± 0.015
$\xi_{{\rm d},49B}$	1.010 ± 0.015	1.011 ± 0.015	1.014 ± 0.015
$\xi_{{\rm p},61}$	1.017 ± 0.019	1.026 ± 0.019	1.028 ± 0.019
$\xi_{{\rm d},61}$	1.004 ± 0.018	1.018 ± 0.018	1.018 ± 0.018
$\xi_{{\rm p},87}$	1.019 ± 0.015	1.029 ± 0.016	1.025 ± 0.015
$\xi_{{\rm d},87}$	1.008 ± 0.015	1.007 ± 0.015	1.011 ± 0.015
$\xi_{{\rm p},89A}$	1.029 ± 0.019	1.057 ± 0.023	1.041 ± 0.020
$\xi_{{\rm d},89A}$	1.005 ± 0.019	1.011 ± 0.020	1.011 ± 0.020
$\xi_{{\rm p},89B}$	1.016 ± 0.015	1.024 ± 0.016	1.021 ± 0.015
$\xi_{{\rm d},89B}$	1.003 ± 0.015	1.004 ± 0.015	1.007 ± 0.015
$\xi_{{\rm d},139}$	1.010 ± 0.015	1.012 ± 0.015	1.014 ± 0.015
χ^2/NDP	1274.3/1243	1248.0/1243	1255.6/1243

Table 4. Correlation coefficients for the parameters of the fit motivated by R_{1990} parametrization

	b_1	b_2	b_3
b_1	1.	-0.61	0.38
b_2	-0.61	1.	-0.87
b_3	0.38	-0.87	1.

$$\left.+\left(1-2\frac{m_l^2}{Q^2}\right)\frac{y^2}{2}\left(F_2^{\rm HT}(x,Q)-F_{\rm L}^{\rm HT}(x,Q)\right)\right],$$

where s is the total c.m.s. energy, m_l is the scattered lepton mass and y is a lepton scattering variable. For testing purposes, we first performed a fit with the $F_{\rm L}$ form moti-

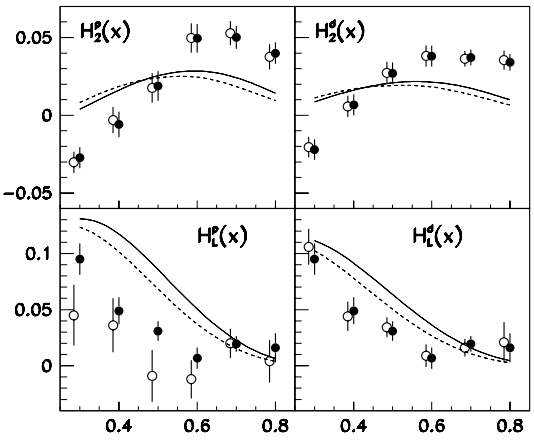

Fig. 2. The values of $H_2(x)$ and $H_{\rm L}(x)$ from the fits with the model-independent form of the HT contribution to $F_{\rm L}$ (empty circles: the unconstrained fit; full circles: the fit with constraint $H_{\rm L}^{\rm d}(x) = H_{\rm L}^{\rm p}(x)$). For a better view, the points are slightly shifted to the left/right along the x axis. The curves are predictions of the infrared renormalon (IRR) model for $Q^2 = 2$ GeV$^2, n_f = 3$ (full lines) and $Q^2 = 9$ GeV$^2, n_f = 4$ (dashed lines)

vated by R_{1990} parametrization [11],

$$F_{\rm L}^{\rm (p,d),HT}(x,Q) = F_2^{\rm (p,d),HT}(x,Q)\left[1 - \frac{1+4M^2x^2/Q^2}{1+R(x,Q)}\right],$$

$$R(x,Q) = \frac{b_1}{2\ln(Q/0.2)}\left[1 + \frac{12Q^2}{Q^2+1}\times\frac{0.125^2}{0.125^2+x^2}\right] + b_2\frac{1\ {\rm GeV}^2}{Q^2} + b_3\frac{1\ {\rm GeV}^4}{Q^4+0.3^2},$$

with fitted parameters $b_{1,2,3}$. This parametrization comprises the term with log-Q behavior, which mimics the LT contribution, and the HT terms with power-Q behavior. The resulting values of the parameters $b_1 = 0.100 \pm 0.042$, $b_2 = 0.46 \pm 0.11$, and $b_3 = -0.14 \pm 0.18$ are in agreement with the values obtained in [11] ($b_1 = 0.064$, $b_2 = 0.57$, $b_3 = -0.35$). In our fit, the twist-6 contribution to $R(x,Q)$ is compatible with zero. We note that the correlations between the parameters are large (see Table 4) and, as a consequence, the data used in the fit have a limited potential, in the separation of both the twist-4/twist-6 and log/power contributions to R.

To achieve more precise determination of the HT contribution to $F_{\rm L}$, one can substitute for the LT contribution a perturbative QCD formula instead of a phenomenological log term. The leading-order QCD gives for the nonsinglet case [18]:

$$F_{\rm L}^{\rm (p,d),LT}(x,Q) = \frac{\alpha_{\rm s}(Q)}{2\pi}\frac{8}{3}x^2\int_x^1\frac{{\rm d}z}{z^3}F_2^{\rm (p,d),LT}(z,Q).$$

We performed the fit using the QCD expression for $F_{\rm L}$ accounting for TMC, i.e.

$$F_{\rm L}^{\rm (p,d),TMC}(x,Q) = F_{\rm L}^{\rm (p,d),LT}(x,Q) + \frac{x^2}{\tau^{3/2}}(1-\tau)\times \frac{F_2^{\rm (p,d),LT}(\xi,Q)}{\xi^2} + \frac{M^2}{Q^2}\frac{x^3}{\tau^2}(6-2\tau)\int_\xi^1 {\rm d}z\frac{F_2^{\rm (p,d),LT}(z,Q)}{z^2}$$

and the additive form of the HT contribution to $F_{\rm L}$, i.e. ,

$$F_{\rm L}^{\rm (p,d),HT}(x,Q) = F_{\rm L}^{\rm (p,d),TMC}(x,Q) + H_{\rm L}^{\rm (p,d)}(x)\frac{1\ {\rm GeV}^2}{Q^2},$$

where $H_{\rm L}^{\rm (p,d)}(x)$ is parametrized in the model-independent form analogously to $H_2^{\rm (p,d)}(x)$ and $h_2^{\rm (p,d)}(x)$. The results of this fit are given in column 2 of Table 3 and in Fig. 2. One can see that with the model-independent parametrization of the HT contribution to $F_{\rm L}$, the renormalization factors for the old SLAC data increase noticeably. We recall that in the source paper [16], these data were renormalized using the data of the dedicated SLAC-E-140 experiment. Since the latter did not report data on the proton target, renormalization of the proton data was performed by the use of bridging through the SLAC-E-49B data. It isn't possible to conclusively choose between our renormalization scheme and the one used in [16]. More proton data are necessary for the adjustment of the old SLAC results. As to the deuterium data, their normalization factors do not practically deviate from 1. The errors of $H_{\rm L}^{\rm d}(x)$, because of the SLAC-E-140 deuterium data, are significantly smaller than for $H_{\rm L}^{\rm p}(x)$. In view of the large errors of the latter, the HT contributions to $F_{\rm L}$ for proton and deuterium are compatible within the errors, and we performed one more fit imposing the constraint $H_{\rm L}^{\rm p}(x) = H_{\rm L}^{\rm d}(x)$. The results of this fit are given in column 3 of Table 3 and in Fig. 2. One can see that χ^2 obtained in this fit is practically equal to the value of χ^2, obtained in the fit without constraints, minus the number of additional parameters. Comparison with Fig. 1 shows that if $F_{\rm L}$ is fitted, the HT contribution to F_2 slightly grows. The value of strong coupling constant decreases if $F_{\rm L}$ is fitted and is insensitive to the constraint imposing, its value

$$\alpha_{\rm s}(M_{\rm Z}) = 0.1170 \pm 0.0021\ ({\rm stat} + {\rm syst}),$$

correspond to

$$\Lambda_{\overline{\rm MS}}^{(3)} = 337 \pm 29\ ({\rm stat} + {\rm syst})\ {\rm MeV},$$

obtained at $Q^2 = 2$ GeV^2 with the help of the relation

$$\alpha_{\rm s}(Q) = \frac{2\pi}{\beta_0\ln(Q/\Lambda)}\Big[1 - \frac{2\pi}{\beta_0\beta}\frac{\ln(2\ln(Q/\Lambda)}{\ln(Q/\Lambda)}\Big],$$

where

$$\beta_0 = 11 - \frac{2}{3}n_f, \quad \beta = \frac{2\pi\beta_0}{51 - \frac{19}{3}n_f}$$

and $n_f = 3$.

We checked how much the analyzed data are sensitive to the twist-6 contribution to $F_{\rm L}$. For this purpose, we fitted to the data $F_{\rm L}(x,Q)$, expressed as

$$F_{\rm L}^{\rm (p,d),HT}(x,Q) = F_{\rm L}^{\rm (p,d),TMC}(x,Q) + H_{\rm L}(x)\frac{1\ {\rm GeV}^2}{Q^2} +$$

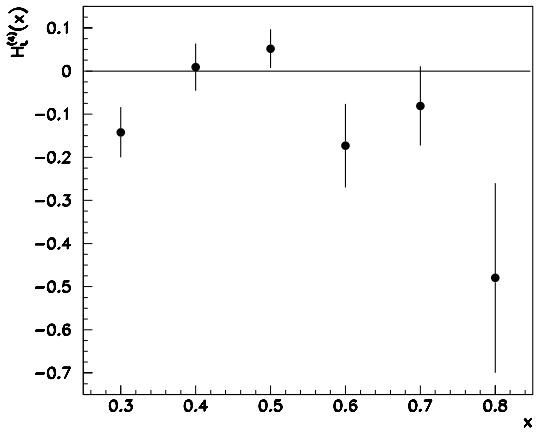

Fig. 3. The dependence of the twist-6 contribution to $F_{\rm L}$ on x

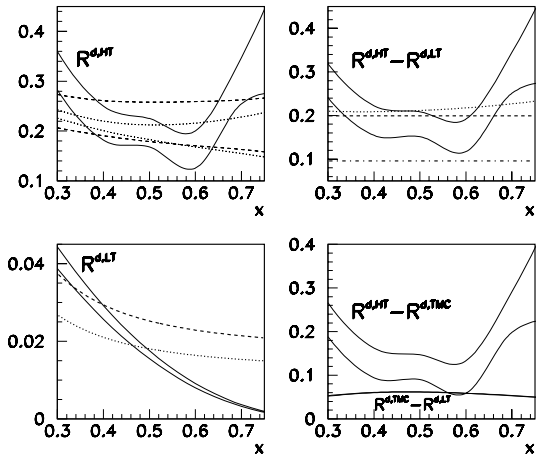

Fig. 4. One-standard-deviation bands for various contributions to our parametrization of $R^{\rm d,HT}(x,Q)$ (full lines). Dashed lines correspond to the R_{1990} parametrization, dotted lines to the R_{1998} one, and dashed–dotted lines to the BRY one [12]. All curves are given for $Q^2 = 2$ GeV^2. Our value of R is obtained as a spline interpolation between the points $x = 0.3, 0.4, 0.5, 0.6, 0.7, 0.8$

$$+H_{\rm L}^{(4)}(x)\frac{1\ \text{GeV}^4}{Q^4},$$

where functions $H_{\rm L}^{(4)}(x)$ and $H_{\rm L}(x)$ were the same for the proton and deuterium and parametrized in the model-independent way. The resulting behavior of $H_{\rm L}^{(4)}(x)$ is given in Fig. 3. One can observe a trend to negative values at highest x, but with a poor statistical significance. The χ^2 decrease in this fit is about 25 (recall that standard deviation of χ^2 is $\sqrt{2\times\text{NDF}}$, i.e., about 40 in our analysis). These results are in correspondence with the estimates of twist-6 contribution to $R(x,Q)$ given above – the fitted twist-6 contribution to $F_{\rm L}$ is at the level of one standard deviation from zero. In our study we did not completely account for the TMC correction of the order $O(M^4/Q^4)$ and so, in a rigorous treatment, $H_{\rm L}^{(4)}$ does not correspond to the pure dynamical twist-6 effects. Meanwhile, the contribution of omitted terms to $H_{\rm L}^{(4)}$ estimated using a formula from [14] does not exceed 0.001 in our region of x and can therefore be neglected.

3 Comparison with other parametrizations

For comparison with other parametrizations, we calculated deuterium $R(x,Q)$ using the relation

$$R^{\rm d,HT}(x,Q) = \frac{F_2^{\rm d,HT}(x,Q)}{F_2^{\rm d,HT}(x,Q)-F_{\rm L}^{\rm d,HT}(x,Q)}\times$$

$$\times\left[1+\frac{4M^2x^2}{Q^2}\right]-1$$

and the parameter values from column 3 of Table 3. The obtained values of R are given in Fig. 4 together with the R_{1990} [11] and R_{1998} [12] parametrizations. On average, all three parametrizations coincide within errors, although our curves lie higher at the edges of the x region and lower in the middle.

The same tendency is valid for the HT+TMC contribution to R, evaluated as a difference between $R^{\rm d,HT}(x,Q)$ and $R^{\rm d,LT}(x,Q)$, where

$$R^{\rm d,LT}(x,Q) = \frac{F_{\rm L}^{\rm d,LT}(x,Q)}{F_2^{\rm d,LT}(x,Q)-F_{\rm L}^{\rm d,LT}(x,Q)}.$$

This contribution is given in Fig. 4 together with the power parts for variants (b) of the $R_{1990,1998}$ parametrizations of [11, 12]. Since error bands are not available for the latter, only the central values are pictured. The relative difference between log parts of the R_{1990} and R_{1998} parametrizations and our $R^{\rm d,LT}(x,Q)$ is very large at highest x, although the absolute difference is not significant, because of the smallness of this term. In Fig. 4, we give the bands for TMC contribution to R, calculated as $R^{\rm d,TMC}-R^{\rm d,LT}$, where

$$R^{\rm d,TMC}(x,Q) = \frac{F_2^{\rm d,TMC}(x,Q)}{F_2^{\rm d,TMC}(x,Q)-F_{\rm L}^{\rm d,TMC}(x,Q)}\times$$

$$\times\left[1+\frac{4M^2x^2}{Q^2}\right]-1,$$

and for the HT contribution, calculated as $R^{\rm d,HT}-R^{\rm d,TMC}$. (Lower and upper bands for the TMC contribution are practically indistinguishable.) It is seen that the TMC contribution is also significantly smaller at large x than the HT one, so the latter is dominating in this region. Meanwhile, we note that as has been observed in [8,19], accounting for NNLO QCD can diminish the value of HT contribution. This effect can be seen in Fig. 4, where we give a power part of the R parametrization [13] obtained with a partial account of NNLO.

In Fig. 5, the data of the SLAC-E140X experiment on nucleon $R(x,Q)$ [20], which were not included in our fit, are compared with $R^{\rm d}(x,Q)$, calculated for the parameter values from column 3 of Table 3. One can observe a good agreement of the data and our parametrization. We also compared the results of the model-independent analysis with predictions of an infrared renormalon model (IRR) [21]. In this model, the HT x-dependence is connected with the LT x-dependence. In particular, for the nonsinglet case, the twist-4 contribution is expressed as

$$H_{2,L}^{\rm (p,d)}(x) = A_2' \int_x^1 {\rm d}z C_{2,L}(z) F_2^{\rm (p,d),LT}(x/z,Q),$$

$$C_2(z) = -\frac{4}{(1-z)_+} + 2(2+z+6z^2) - 9\delta(1-z) - \delta'(1-z),$$

$$C_{\rm L}(z) = 8z^2 - 4\delta(1-z),$$

$$A_2' = -\frac{2C_F}{\beta_0}\left[\Lambda_R\right]^2 {\rm e}^{-C},$$

where $C_{\rm F} = 4/3$, $C = -5/3$. The normalization factor $\Lambda_{\rm R}$ can be considered as a fitted parameter, or, in another approach, set equal to the value of $\Lambda_{\rm QCD}$. In Fig. 2, we give the IRR model predictions at $\Lambda_R = \Lambda^{(3)}_{\overline{\rm MS}} = 337$ MeV, as obtained in our analysis. Parameters of LT structure functions were taken from column 2 of Table 3. One can see that the model qualitatively describes the $H_{\rm L}(x)$ data. This in agreement with the curves given in Fig. 6 of [22] (recall that our value of Λ is about 1.3 times larger than one used in [22] to calculate these curves). At the same time, there is evident discrepancy between the model and the $H_2(x)$ data. It should be noted that $H_2(x)$ is strongly correlated with other parameters, and, in particular, with $\alpha_{\rm s}(M_{\rm Z})$. In Table 5, we give global correlation coefficients ρ_m, calculated as

$$\rho_m = \sqrt{1 - 1/e_{mm}/c_{mm}},$$

where c_{mn} is the parameter error matrix, e_{mn} is its inverse, and indices m,n run through the fitted parameters. The global coefficients characterize the extent of correlation of a parameter with all other parameters. (For the two parameters fit $\rho_1 = \rho_2$ and both are equal to the correlation coefficient between these parameters). From Table 5, one can see that $H_{\rm L}$ is almost uncorrelated with $\alpha_{\rm s}(M_{\rm Z})$ and is correlated with other parameters less than H_2. This fact can be readily understood qualitatively. The total value of $R^{\rm HT}$ is defined from the y dependence of cross sections and is weakly correlated with $\alpha_{\rm s}$. Then, the correlation of $H_{\rm L}$ with $\alpha_{\rm s}$ can arise only from the dependence of LT contribution on $\alpha_{\rm s}$. Since the LT contribution is small as compared with the HT one (see Fig. 4), this dependence does not cause significant correlations of the HT contribution and $\alpha_{\rm s}$. Owing to the lower values of ρ, $H_{\rm L}$ is more stable in respect with the change of ansatz and input of the fit. The shift of $\alpha_{\rm s}$ towards higher values would not affect $H_{\rm L}$, but can decrease H_2.

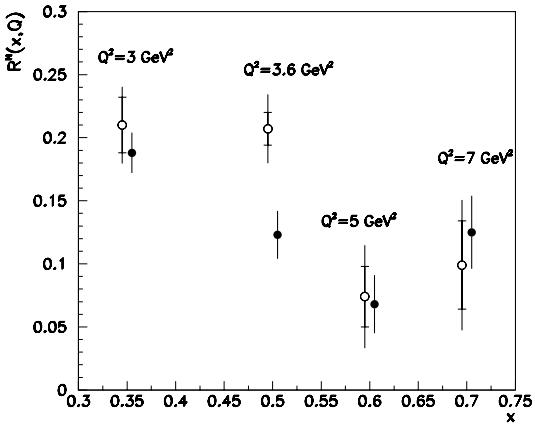

Fig. 5. The E140X data on nucleon $R(x,Q)$ (empty circles). Inner bars correspond to statistic errors, total bars to statistic and systematic ones combined in quadrature. Also given are the calculations of deuterium $R(x,Q)$ performed on our parametrization (full circles). For a better view, the points are slightly shifted to the left/right along the x axis

Table 5. The correlation coefficients for HT parameters and $\alpha_{\rm s}(M_{\rm Z})$. Figures in parentheses are the global correlation coefficients for HT parameters

x	$H_2^{\rm p}(x)$	$H_2^{\rm d}(x)$	$H_{\rm L}(x)$
0.3	-0.507(0.914)	-0.707(0.964)	-0.029(0.868)
0.4	-0.847(0.955)	-0.910(0.976)	0.122(0.852)
0.5	-0.909(0.968)	-0.944(0.987)	0.244(0.870)
0.6	-0.905(0.971)	-0.917(0.977)	0.222(0.866)
0.7	-0.871(0.972)	-0.901(0.980)	0.072(0.894)
0.8	-0.460(0.868)	-0.429(0.875)	0.156(0.870)

4 Conclusion

We have performed the NLO QCD fit to the combined SLAC-BCDMS-NMC DIS data at high x. The model-independent x shape of high-twist contribution to structure function $F_{\rm L}$ is extracted. The twist-4 contribution to $F_{\rm L}$ is found to be in qualitative agreement with the predictions of the infrared renormalon model. The twist-6 contribution exhibits a weak trend to negative values, although on the whole, it is compatible with zero within the errors.

Acknowledgements. I am indebted to A.L. Kataev, G. Marchesini, and E. Stein for discussions and valuable comments.

References

1. M. Virchaux, A. Milsztajn, Phys. Lett. B **274**, 221 (1992)
2. A.V. Kotikov, V.G. Krivokhijine, hep-ph/9805353, 1998
3. S.I. Alekhin, Phys. Rev. D **59**, 114016 (1999)
4. NM Collaboration: M. Arneodo, et al., Phys. Lett. B **309**, 222 (1993)

5. BCDMS Collaboration: A.C. Benvenuti, et al., Phys. Lett. B **223**, 485 (1989);
BCDMS Collaboration: A.C. Benvenuti, et al., Phys. Lett. B **237**, 592 (1990)
6. L.W. Whitlow, et al., Phys. Lett. B **282**, 475 (1992)
7. NM Collaboration: M. Arneodo, et al., Nucl. Phys. B **483**, 3 (1997)
8. A.L. Kataev, A.V. Kotikov, G. Parente, A.V. Sidorov, Phys. Lett. B **417**, 374 (1998); A.L. Kataev, G. Parente, A.V. Sidorov, Report No. INR-P089/98, hep- ph/9809500
9. S.I. Alekhin, A.L. Kataev, Phys. Lett. B **452**, 402 (1999)
10. CCFR Collaboration: W.G. Seligman, et al., Phys. Rev. Lett. **79**, 1213 (1997)
11. L.W. Whitlow, et al., Phys. Lett. B **250**, 193 (1990)
12. E143 Collaboration: K. Abe, et. al., Phys. Lett. B **452**, 194 (1999)
13. A. Bodek, S. Rock, U. Yang, UR-1355, 1996
14. H. Georgi, H.D. Politzer, Phys. Rev. D **14**, 1829 (1976)
15. S.I. Alekhin, Eur. Phys. J. C **10**, 395 (1999)
16. L.W. Whitlow, SLAC-Report-357, 1990
17. G. Ricco, S. Simula, M. Battaglieri, INFN-RM3 98-2, hep-ph/9901360, 1999
18. G. Altarelli, G. Martinelli, Phys. Lett. B **76**, 89 (1978)
19. U.K. Yang, A. Bodek, Phys. Rev. Lett. **82**, 2467 (1999)
20. E140X Collaboration: L.H. Tao, et. al., Z. Phys. C **70**, 387 (1996)
21. Yu.L. Dokshitzer, G. Marchesini, B.R. Webber, Nucl. Phys. B **469**, 93 (1996); E. Stein, M. Meyer-Hermann M, A. Schäfer, L. Mankiewicz, Phys. Lett. B **376**, 177 (1996); M. Dasgupta, B.R. Webber, Phys. Lett. B **382**, 273 (1996)
22. E. Stein, M. Maul, L. Mankiewicz, A. Schäfer, DFTT-13-97, TPR-98-13, TUM/T39-98-8, hep-ph/9803342, 1998